Electronic supplementary information for "Nonequilibrium phase diagrams for actomyosin networks"

Simon L. Freedman, Glen M. Hocky, Shiladitya Banerjee, Aaron R. Dinner

S1   AFINES simulation

In AFINES, actin filaments, myosin motors, and passive crosslinkers are modeled as coarse-grained entities. Actin filaments are treated as worm-like chains of $N + 1$ beads connected by N harmonic springs (links) and $N - 1$ angular harmonic springs. Thus, the internal forces on an actin filament can be obtained from the gradient of the potential energy U_f:

$$U_f = \frac{k_a}{2} \sum_{i=1}^{N} (|\vec{r}_i - \vec{r}_{i-1}| - l_a)^2 + \frac{\kappa_B}{2l_a} \sum_{i=2}^{N} \theta_i^2, \tag{S1}$$

where $\vec{r}_i$ is the position of the ith bead on a filament, θ_i is the angle between the ith and $(i-1)^{th}$ links, k_a is the stretching force constant, κ_B is the bending modulus, and l_a is the equilibrium length of a link. The persistence length of the filament is then $L_p = \kappa_B/k_B T$, where k_B is Boltzmann's constant and T is the temperature.

We model crosslinkers as Hookean springs, with two ends (heads) that can stochastically bind to and unbind from filaments. Thus, the potential energy of a crosslinker is

$$U_{xl} = \frac{1}{2} k_{xl} (|\vec{r}_1 - \vec{r}_2| - l_{xl})^2 - k_B T \ln (k_{xl}^{\text{on}}/k_{xl}^{\text{off}})(I_1 + I_2), \tag{S2}$$

where k_{xl} is the crosslinker stiffness, l_{xl} is its rest length, $\vec{r}_{1(2)}$ is the position of head 1(2), $I_{1(2)}$ is 1 if head 1(2) is bound and 0 otherwise, and $k_{xl}^{\text{on}}(k_{xl}^{\text{off}})$ is the rate constant for binding (unbinding). When a crosslinker is bound, it moves with the filament to which it is bound. When both crosslinker heads are bound, its tensile force, $\vec{F}_{xl}$ is propagated onto the filament beads neighboring each bound head at position $\vec{r}_{xl}$ via the lever rule,

$$\vec{F}_i = \vec{F}_{xl} \frac{|\vec{r}_{i+1} - \vec{r}_{xl}|}{|\vec{r}_{i+1} - \vec{r}_i|} \quad \text{and} \quad \vec{F}_{i+1} = \vec{F}_{xl} - \vec{F}_i, \tag{S3}$$

where $\vec{F}_i$ is the force on the filament bead at position $\vec{r}_i$.

Binding and unbinding are governed by a Monte Carlo procedure constructed to satisfy detailed balance in the absence of motors. At each timestep of duration Δt, an unbound crosslinker head becomes bound to the ith nearby filament with probability $k_{xl}^{\text{on}} \Delta t P_i$, where P_i is defined as follows. The closest point on the filament is identified, and the change in energy

associated with moving the head to it, ΔU_i is computed; $P_i = \min\left[1, \exp\left(-\Delta U_i/k_B T\right)\right]$. When a head becomes bound, its displacement, in the frame of reference of the filament link to which it attached, is stored as $\Delta \vec{r}$. Later, the head can become unbound and displaced $-\Delta \vec{r}$ with probability $k_{xl}^{\text{off}} \Delta t P$, where $P = \min\left[1, \exp(-\Delta U/k_B T)\right]$ and ΔU is the energy associated with the displacement. Because the dynamics depend on the allowed moves in the Monte Carlo procedure, care must be used in interpreting the values of the rate constants. That said, the values that we obtain by tuning the parameters to yield behaviors consistent with experiments are generally within an order of magnitude of measured rate constants.

We model motors similarly to crosslinkers, in that they are Hookean springs, can bind to and unbind from filaments, and propagate force onto them. Thus, their potential energy is identical to Eq. S2 with the subscript m replacing the subscript xl. Additionally, a bound motor head moves towards the barbed end of the actin filament to which it is bound at a load-dependent velocity

$$v(F_m) = v_0 \max\left[1 + \frac{\vec{F}_m \cdot \hat{r}}{F_s}, 0\right], \tag{S4}$$

where v_0 is the unloaded motor speed, $\vec{F}_m = -k_m(|\vec{r}_1 - \vec{r}_2| - l_m)$ is the tensile force on the motor, and $\hat{r}$ is the tangent to the filament at the point where the motor is bound; $\hat{r}$ points toward the pointed end of the filament.

We simulate the system using Brownian dynamics such that the position of an actin bead, motor head, or crosslinker head at time t is generated by the equation

$$\vec{r}(t + \Delta t) = \vec{r}(t) + \vec{F}(\vec{r}(t))\mu\Delta t + \sqrt{\frac{k_B T \mu \Delta t}{2}}\left(\vec{W}(t + \Delta t) + \vec{W}(t)\right), \tag{S5}$$

where $\vec{F}(\vec{r}(t))$ is the gradient of the potential of the particle, $\vec{W}(t)$ is a vector of random numbers drawn from the standard normal distribution, and we use the Stokes relation $\mu = 1/(6\pi R \nu)$ in the damping term, where R is the size of the particle, and ν is the dynamic viscosity of its environment [S1]. We simulate the system in 2D and use periodic boundary conditions to limit boundary effects. A complete list of model parameters used for Figures 1, 2, 4 and 5 is provided in Table S1 and additional methods used for Fig. 7 are described below (Section S3).

| Symbol	Description (units) [ref]	Value
	Actin Filaments	
ρ_l	link density (μm^{-2})	2
N_l	number of links per filament (L/l_a)	$[1, 15]$
l_a	link rest length (μm) [S2]	1
k_a	stretching force constant (pN/μm)	5
κ_B	bending modulus (pNμm^2) [S3]	0.068
	Myosin Minifilaments	
ρ_m	density (μm^{-2})	$[0, 0.3]$
l_m	rest length (μm) [S4]	0.5
k_m	stiffness (pN/μm)	1
k_m^{on}	maximum attachment rate (s^{-1})	1
k_m^{off}	maximum detachment rate (s^{-1})	$[0.01, 1]$
k_m^{end}	maximum end detachment rate (s^{-1})	$[0.01, 1]$
v_0	unloaded speed (μm/s) [S5]	1
F_s	stall force of myosin (pN) [S6]	0.5
	Crosslinkers	
ρ_{xl}	density (μm^{-2})	$[0, 1.5]$
l_{xl}	rest length (filamin) (μm) [S7]	0.15
k_{xl}	stiffness (pN/μm)	1
k_{xl}^{on}	maximum attachment rate (s^{-1})	1
k_{xl}^{off}	maximum detachment rate (s^{-1})	$[0.01, 1]$
	Environment	
Δt	dynamics timestep (s)	0.00002
t_F	maximum simulated time (s)	400
X, Y	length and width of assay (μm)	50
g	grid density (μm^{-1})	2.5
T	temperature (K)	300
ν	dynamic viscosity (Pa·s)	0.001

Table S1: Parameter Values
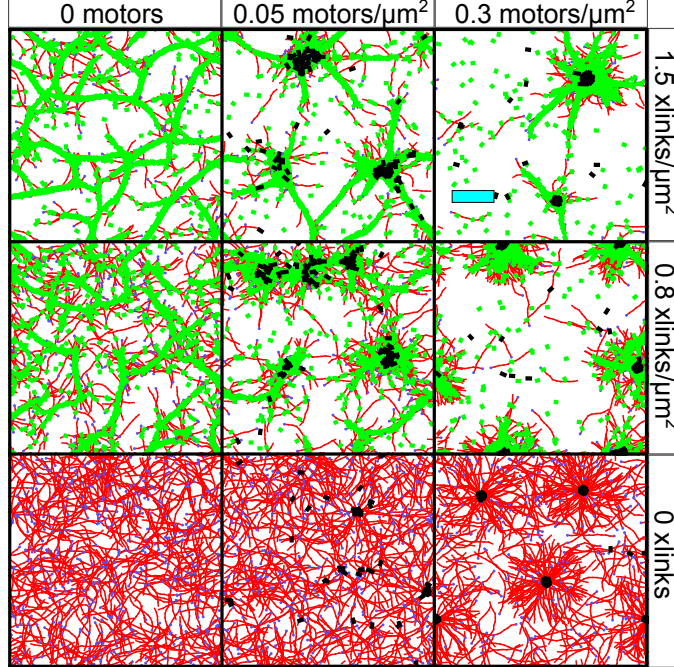
Figure S1: Same as Fig. 1, but with motors (black) and crosslinkers (green) also shown on top of actin (red, barbed ends marked by blue dots). Cyan scale bar is 10 μm. Parameters held constant: $L = 10$ μm, $k^{\text{off}}_{xl(m)} = 0.1$ s^{-1}.

S2   Order parameter calculation details

S2.1   Radial distribution function

To measure the radial distribution function, we use the 2D, single-timestep analog of Eq. 6.3 in [S8]:

$$g(r + \delta r/2) = \frac{2n(r)A}{\pi\left((r + \delta r)^2 - r^2\right)N^2},$$
(S6)

where $n(r)$ is the number of distances between particles in the interval $[r, r + \delta r]$, A is the area of the simulation cell, N is the total number of particles, and $\rho = N/A$. The total number of distances between particles is $n = N(N-1)/2 \approx N^2/2$ for large N, and distances are typically large compared to the bin width (i.e., $\delta r \ll r$), yielding the simplified form shown in Eq. 1:

$$g(r) = \frac{P(r)A}{2\pi r \delta r}.$$
(S7)

Above, we have substituted $P(r) = n(r)/n$ as the probability of distance r. We found that $P(r)$ was well approximated by randomly sampling $\sim$10,000 distances between particles.

S2.2   Divergence of actin velocity field

Contraction of actin networks is typically calculated by identifying sinks in the divergence of the actin velocity field. To construct this field, we first calculate the velocity of actin beads $\vec{v}_a = (\vec{r}_a(t+h) - \vec{r}_a(t))/h$ where $\vec{r}_a(t)$ is the position of an actin bead at time t, and h is the lag time. To reduce noise, we calculate $\vec{v}_k(\vec{r}_k)$, the average velocity in every bin k of size Δr^2. We then interpolate the velocity field using Gaussian radial basis functions (RBFs), such that the velocity at any position $\vec{r}$ is

$$\vec{v}(\vec{r}) = \sum_{k=1}^{M} \vec{w}_k e^{-(|\vec{r}-\vec{r}_k|/\epsilon)^2}, \tag{S8}$$

where M is the number of bins with at least 10 actin beads, and $\vec{w}_k$ are the weights of the basis functions, determined by solving the equation $\vec{v}(\vec{r}_k) = \vec{v}_k(\vec{r}_k)$ (using the scipy.interpolate.Rbf package [S9]). For Fig. 2B, we used a lag time of $h = 10$ s, a threshold of $n = 10$ actin beads in a local box of size $\Delta r = 5$ μm, and a Gaussian width of $\epsilon = 5$ μm, as we have found these interpolation values robustly capture the motion of the actin [S10].

Because of the periodic boundary conditions, there is no flux of actin into the simulation cell, and $\langle \nabla \cdot \vec{v}(r) \rangle = 0$. Therefore, to measure contraction, we threshold the divergence by the local actin density and only total the divergence from 1 μm^2 patches that contain more than 5 actin beads in Fig. 2D, as in Ref. S11.
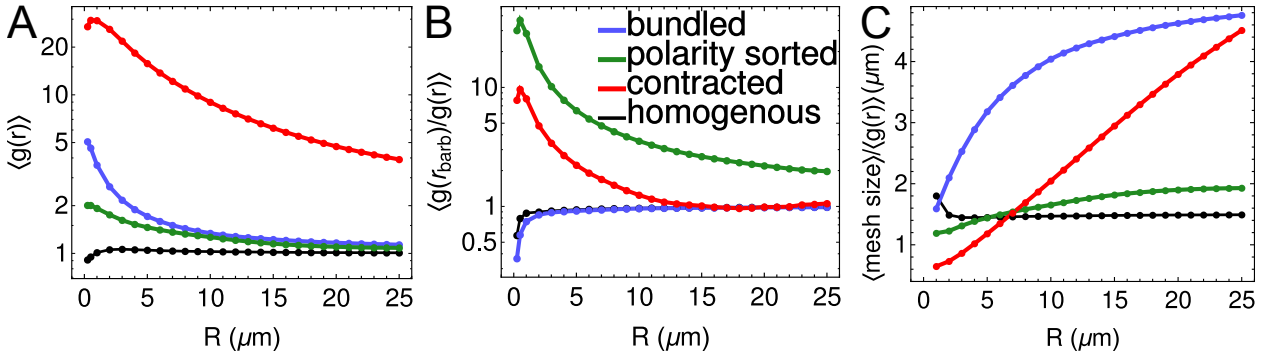

Figure S2: Variation of order parameters with R, the upper integration limit for $\langle g(r) \rangle$ and $\langle g(r_{barb}) \rangle$. Since the length and width of the periodic simulation cell is 50 μm, the largest unambiguous distance is half that, 25 μm. (A) For all values of R, $\langle g(r) \rangle$ is highest for contracted networks, followed by bundled networks. (B) For all values of R, $\langle g(r_{barb})/g(r) \rangle$ is highest for polarity-sorted networks, followed by contracted networks. (C) For $R > 1$ μm, $\langle$mesh size$/g(r) \rangle$ is highest for bundled networks, consistently followed by contracted networks for $R \geq 8$ μm.
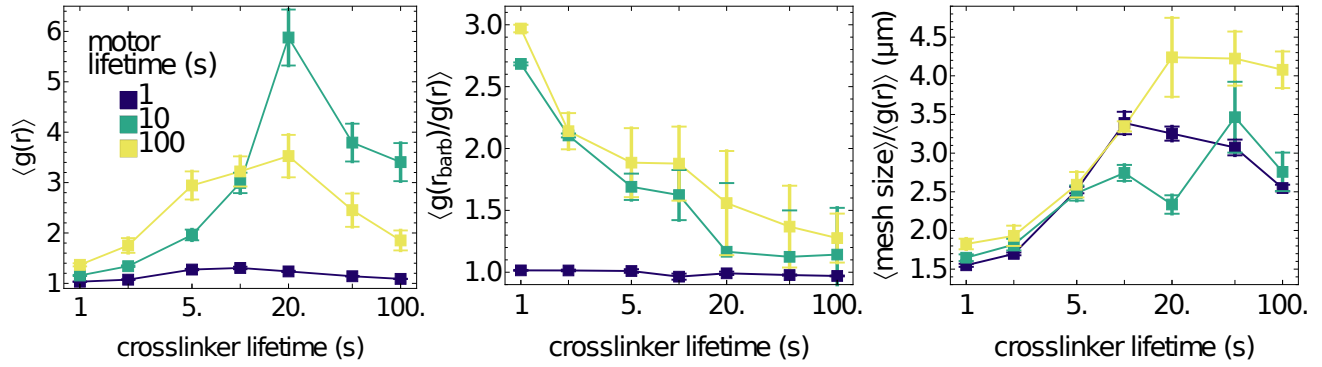
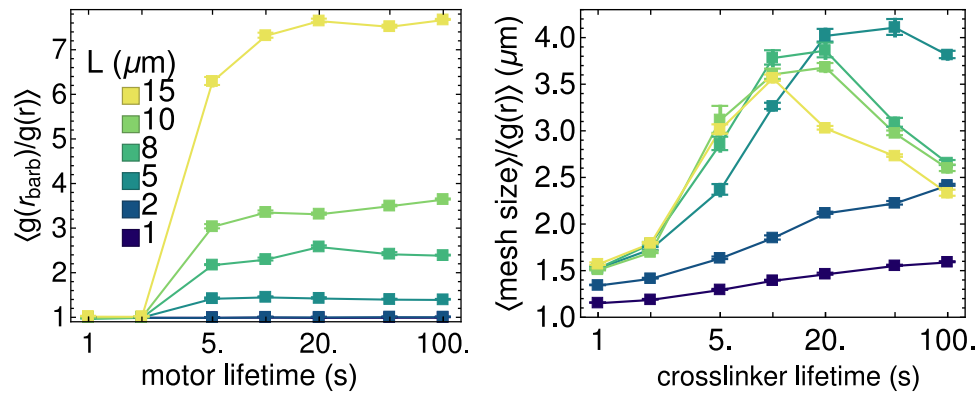Figure S3: Example cuts from Fig. 4D-F to show typical sizes of standard errors of the means.

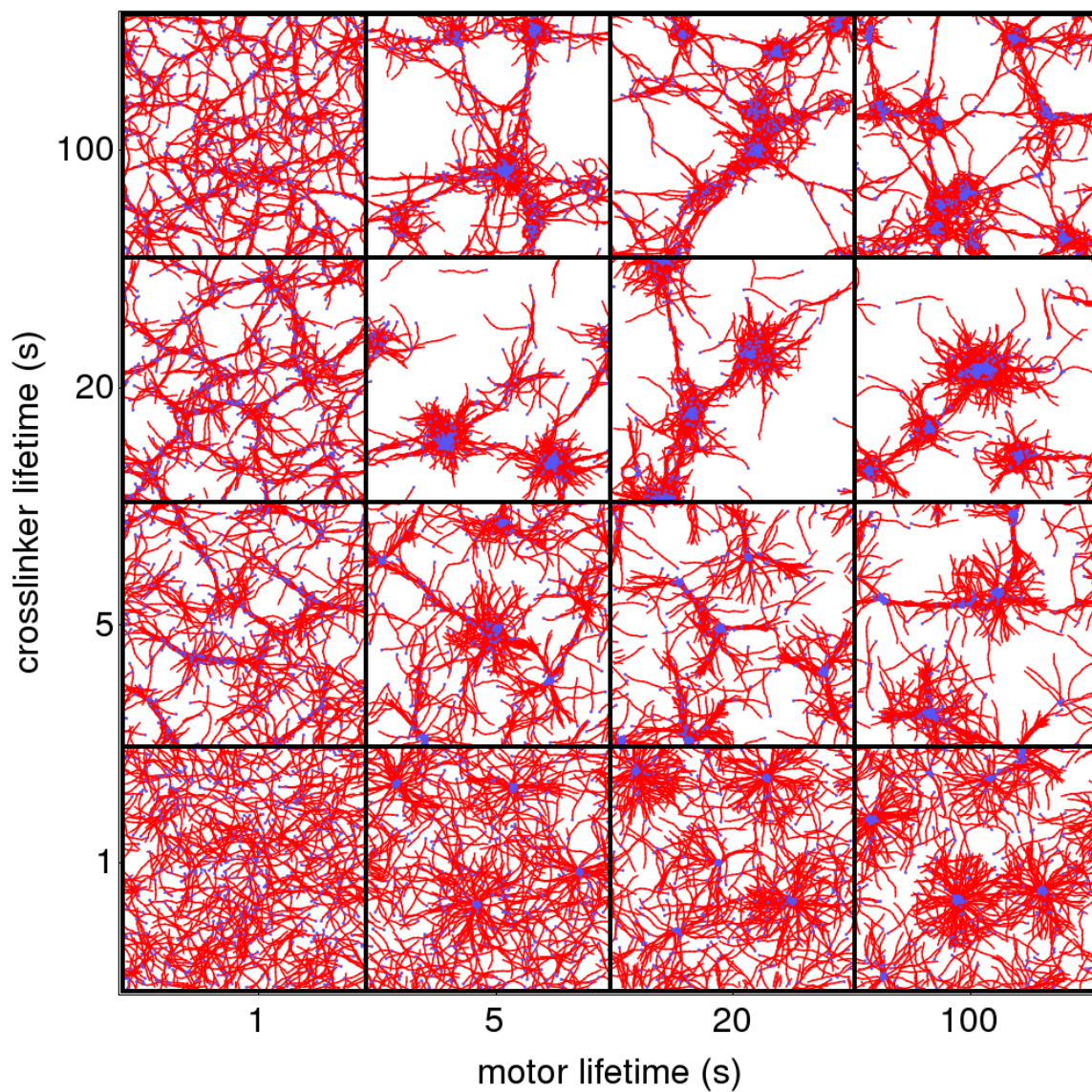Figure S4: Same as Fig. 5B-C but normalized by $\langle g(r) \rangle$.

Figure S5: Sample structures after 400 s simulation, for varying motor and crosslinker off rates. Parameters held constant: $\rho_m = 0.2 \ \mu\mathrm{m}^{-2}$, $\rho_{xl} = 1 \ \mu\mathrm{m}^{-2}$, $L = 10 \ \mu\mathrm{m}$. Motors and crosslinkers not shown for clarity.
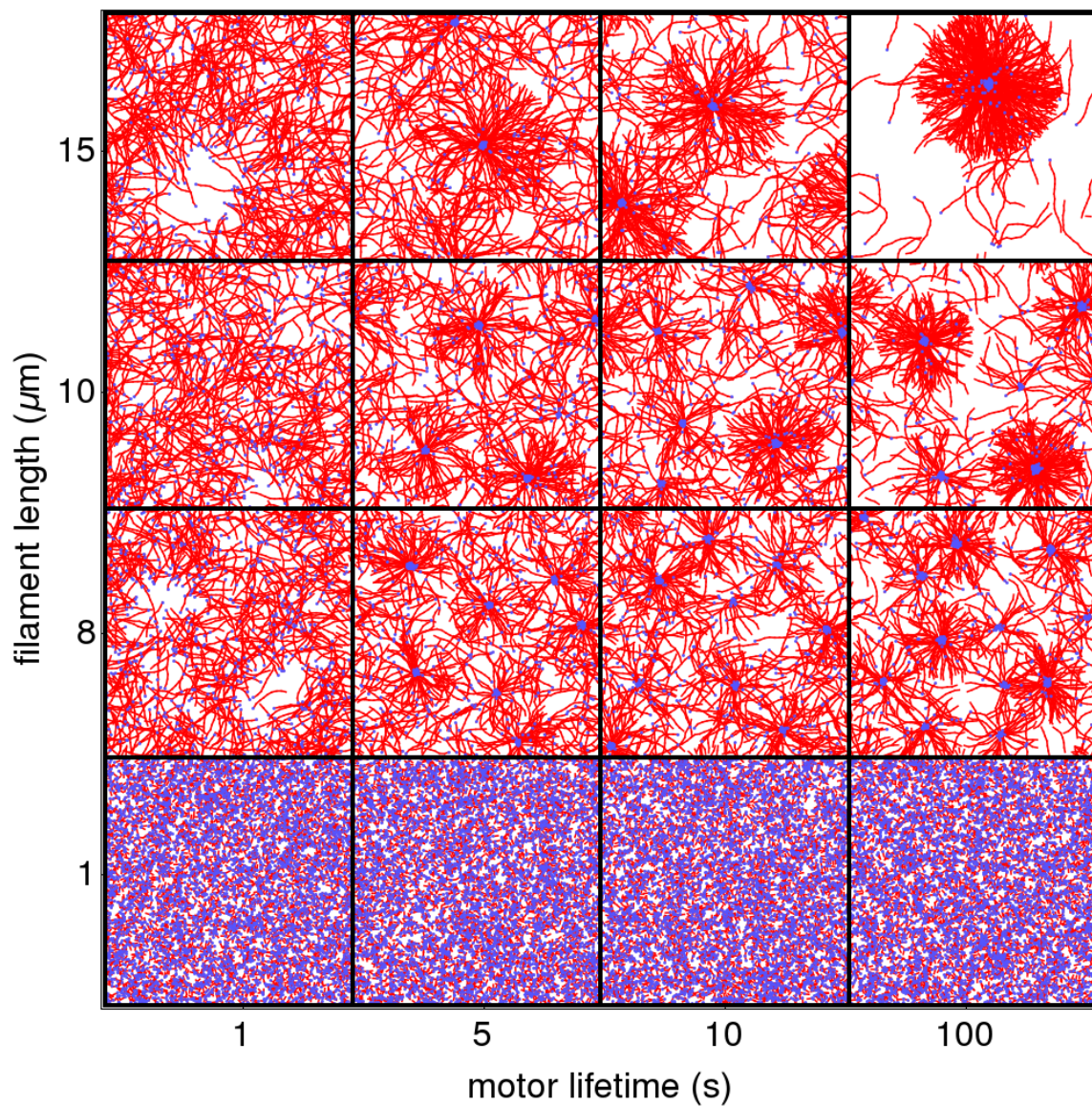
Figure S6: Sample structures after 400 s simulation, for varying filament length and motor off rate. Parameters held constant: $\rho_m = 0.3\ \mu\text{m}^{-2}$, $\rho_{xl} = 0$. Motors and crosslinkers not shown for clarity.
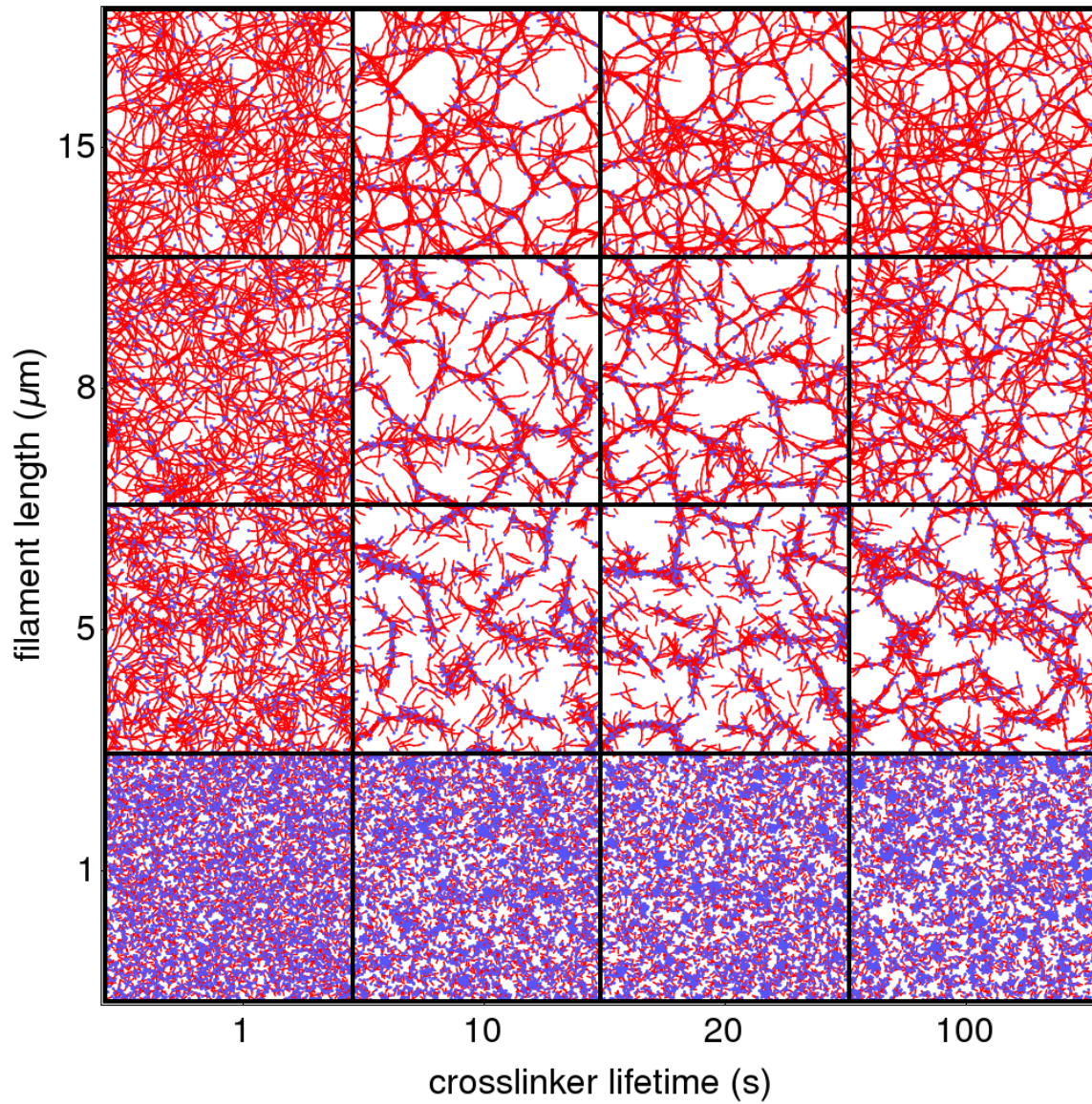
Figure S7: Sample structures after 400 s simulation, for varying filament length and crosslinker off rate. Parameters held constant: $\rho_m = 0$, $\rho_{xl} = 1.5$ μm^{-2}. Motors, crosslinkers, and barbed ends not shown for clarity.

S3 Simulating shear

To measure the stiffness of self-assembled actin networks, we simulate a controlled strain experiment and shear the final network configuration by a total strain of $\gamma = 0.5$ in a fixed amount of time $t_F = 0.5$ s. This is accomplished by supplementing the Brownian dynamics described in Section S1 by explicitly shifting the actin bead position (x_i, y_i) such that $x_i \to x_i + \gamma(dt/t_F)(y_i/Y)$ where Y is the simulation cell height, and dt is the amount of time for a small shear [S12]. Additionally, the boundary conditions follow the Lees-Edwards convention during the shear [S13]. As described in [S10], we do not perform this shift at every time step; rather $dt = \Delta t + t_{relax}$ where Δt is the simulation time step and t_{relax} is a suitable amount of time for the simulation to relax from the large external force imposed by the shear. In Fig. 2F, we used $\Delta t = 10^{-7}$ s and $dt = 10^{-3}$ s.

The viscoelastic response of a network undergoing simple shear is typically measured by computing the stress σ on the network as a function of the strain γ. In general, this response is frequency dependent, such that if the system is sheared sinusoidally, with a frequency of ω, then the expected stress response is

$$\sigma = G'(\omega)\gamma + G''(\omega)\dot{\gamma}/\omega \tag{S9}$$

where $G'(\omega)$ is the storage modulus, $G''(\omega)$ is the loss modulus, and $\dot{\gamma}$ is the strain rate. At long times, or for a constant strain ($\omega \to 0$), $G'(\omega)$ is the shear modulus of the material, and $G''(\omega)/\omega$ is its dynamic viscosity. Additionally, because for 2D networks the stress is not well defined, we instead measure the energy density $w(\gamma)$, as it satisfies the equation $dw/d\gamma = \sigma$. Integrating Eq. S9 with respect to γ and substituting the constant-strain approximation, we obtain our model $w(\gamma) = 1/2G\gamma^2 + \eta\dot{\gamma}\gamma + w(0)$ [S14].

References

[S1] Benedict Leimkuhler and Charles Matthews. Robust and efficient configurational molecular sampling via langevin dynamics. *J. Chem. Phys.*, 138(17):174102, 2013.

[S2] Theo Odijk. The statistics and dynamics of confined or entangled stiff polymers. *Macromolecules*, 16(8):1340–1344, 1983.

[S3] A. Ott, M. Magnasco, A. Simon, and A. Libchaber. Measurement of the persistence length of polymerized actin using fluorescence microscopy. *Phys. Rev. E*, 48:R1642–R1645, Sep 1993.

[S4] Richard Niederman and Thomas D. Pollard. Human platelet myosin ii in vitro assembly and structure of myosin filaments. *J. Cell Biol.*, 67(1):72–92, 1975.

[S5] Stephen J. Kron and James A. Spudich. Fluorescent actin filaments move on myosin fixed to a glass surface. *Proc. Natl. Acad. Sci. USA*, 83(17):6272–6276, 1986.

[S6] Claudia Veigel, Justin E. Molloy, Stephan Schmitz, and John Kendrick-Jones. Load-dependent kinetics of force production by smooth muscle myosin measured with optical tweezers. *Nat. Cell Biol.*, 5(11):980–986, 2003.

[S7] Jorge M. Ferrer, Hyungsuk Lee, Jiong Chen, Benjamin Pelz, Fumihiko Nakamura, Roger D. Kamm, and Matthew J. Lang. Measuring molecular rupture forces between single actin filaments and actin-binding proteins. *Proc. Natl. Acad. Sci. USA*, 105(27):9221–9226, 2008.

[S8] Mike P. Allen and Dominic J. Tildesley. *Computer Simulation of Liquids*. Oxford University Press, New York, NY, 1989.

[S9] Robert Hetland and John Travers. SciPy: Open source scientific tools for Python: rbf - radial basis functions for interpolation/smoothing scattered nd data, 2001.

[S10] Simon L Freedman, Shiladitya Banerjee, Glen M Hocky, and Aaron R Dinner. A versatile framework for simulating the dynamic mechanical structure of cytoskeletal networks. *Biophys. J*, 113(2):448–460, 2017.

[S11] Samantha Stam, Simon L. Freedman, Shiladitya Banerjee, Kimberly L. Weirich, Aaron R. Dinner, and Margaret L. Gardel. Filament rigidity and connectivity tune the deformation modes of active biopolymer networks. *Proc. Natl. Acad. Sci. U.S.A*, 114(47):E10037–10045, 2017.

[S12] Denis J. Evans and G. P. Morriss. Nonlinear-response theory for steady planar couette flow. *Phys. Rev. A*, 30:1528–1530, Sep 1984.

[S13] AW Lees and SF Edwards. The computer study of transport processes under extreme conditions. *J. Phys. C: Solid State Phys.*, 5(15):1921, 1972.

[S14] David H Boal. *Mechanics of the Cell*. Cambridge University Press, 2012.